Development 138, 4193-4198 (2011) doi:10.1242/dev.065375

Transmembrane protein 2 (Tmem2) is required to regionally restrict atrioventricular canal boundary and endocardial cushion development

Kelly A. Smith[1,2,*], Anne K. Lagendijk[1], Andrew D. Courtney[2], Huijun Chen[2], Scott Paterson[2], Benjamin M. Hogan[2], Carol Wicking[2] and Jeroen Bakkers[1,3,*]

SUMMARY

The atrioventricular canal (AVC) physically separates the atrial and ventricular chambers of the heart and plays a crucial role in the development of the valves and septa. Defects in AVC development result in aberrant heart morphogenesis and are a significant cause of congenital heart malformations. We have used a forward genetic screen in zebrafish to identify novel regulators of cardiac morphogenesis. We isolated a mutant, named *wickham* (*wkm*), that was indistinguishable from siblings at the linear heart tube stage but exhibited a specific loss of cardiac looping at later developmental stages. Positional cloning revealed that the *wkm* locus encodes transmembrane protein 2 (Tmem2), a single-pass transmembrane protein of previously unknown function. Expression analysis demonstrated myocardial and endocardial expression of *tmem2* in zebrafish and conserved expression in the endocardium of mouse embryos. Detailed phenotypic analysis of the *wkm* mutant identified an expansion of expression of known myocardial and endocardial AVC markers, including *bmp4* and *has2*. By contrast, a reduction in the expression of *spp1*, a marker of the maturing valvular primordia, was observed, suggesting that an expansion of immature AVC is detrimental to later valve maturation. Finally, we show that immature AVC expansion in *wkm* mutants is rescued by depleting Bmp4, indicating that Tmem2 restricts *bmp4* expression to delimit the AVC primordium during cardiac development.

KEY WORDS: Forward genetics, Atrioventricular canal, Tmem2, Zebrafish

INTRODUCTION

During mammalian embryonic development, the primitive linear heart tube undergoes dynamic morphogenesis to give rise to the looped heart. This process begins as an asymmetric positioning of the heart tube followed by subsequent ballooning of the developing chambers and constriction of the atrioventricular canal (AVC). The AVC partitions the atrial and ventricular chambers and gives rise to the endocardial cushions (ECs), which later contribute to the developing valves and septa of the heart. The AVC remains in an undifferentiated state, in contrast to the differentiating chamber myocardium, and employs a defined genetic programme to establish and maintain this spatially discrete region (Moorman and Christoffels, 2003). Developmental defects arising from improper AVC formation give rise to atrioventricular septal defects. These malformations constitute the largest subset of human congenital heart malformations and can have devastating consequences for the affected individual (Lagendijk et al., 2010). Identifying and characterising the molecular regulators of AVC development are crucial to understanding and managing this group of diseases.

For more than a decade, the zebrafish has successfully been used as a model with which to identify regulators of cardiac morphogenesis, including the AVC. Mutants for genes such as *ugdh* (*jekyll*) (Walsh and Stainier, 2001), *notch1* (Timmerman et al., 2004) and *foxn4* (*slipjig*) (Chi et al., 2008) exhibit a loss or diminution of EC development. By contrast, mutations in *apc* (Hurlstone et al., 2003), *tbx5* (*heartstrings*) (Camarata et al., 2010; Garrity et al., 2002) or *hey2* (*gridlock*) (Rutenberg et al., 2006) result in an expansion of the AVC. In this latter category of mutants, the AVC-chamber boundary is compromised. Although the AVC defects in these mutants are phenotypically and molecularly diverse, each case is accompanied by cardiac looping defects, suggesting that appropriate patterning of the AVC is essential for correct looping and morphogenesis of the heart.

Here, we describe a novel zebrafish mutant, *wickham* (*wkm*), identified in a forward genetic screen by a defect in cardiac looping. We show that the *wkm* mutant harbours a mutation in *tmem2*, a previously undescribed regulator of cardiac development that is expressed in the zebrafish and mammalian heart.

MATERIALS AND METHODS

Fish and mouse lines and fish mutagenesis

Fish were kept under standard conditions as previously described (Westerfield, 1995). The *tg(myl7:dsRed)* and *tg(kdrl:gfp)* lines were described previously (Huang et al., 2003; Lawson and Weinstein, 2002; Mably et al., 2003). Pregnant wild-type CD1 mice were sacrificed and embryos dissected at the required stages.

ENU mutagenesis was performed as previously described (Wienholds et al., 2002). F1 progeny from mutagenised Tuebingen Longfin males were crossed to an AB strain to produce F2 families. Subsequent incrossing of F2 progeny generated F3 embryos that were screened for cardiac morphogenesis defects. All animal work conformed to ethical guidelines and was approved by the relevant animal ethics committees at the Hubrecht Institute and the University of Queensland.

Positional cloning of *wkm*

The *tmem2*^{hu4800} allele was mapped using standard meiotic mapping with simple sequence length polymorphisms (SSLPs). Unique SSLP primer sequences for the region (CA1-CA4) are listed in Table S1 in the

[1]Hubrecht Institute, KNAW and University Medical Center Utrecht, 3584 CT Utrecht, The Netherlands. [2]Institute for Molecular Bioscience, The University of Queensland, Brisbane, Queensland 4072, Australia. [3]Interuniversity Cardiology Institute of the Netherlands, 3501 DG Utrecht, The Netherlands.

*Authors for correspondence (k.smith@imb.uq.edu.au; j.bakkers@hubrecht.eu)

Accepted 2 August 2011

supplementary material. Linkage for the *tmem2*^{hu5935} allele was also performed using SSLP markers. Subsequent genotyping of the *tmem2*^{hu5935} allele was performed by sequencing using the primer pair 5′-ATGTCTTGGACCTTCCTCAC-3′ (forward) and 5′-AGAACAGAGTATAAAGCCCTCTG-3′ (reverse). The genomic region was analysed with reference to Ensembl assembly zv8, release 55, December 2008.

Probe sequence and morpholino Injections

A 1500 bp fragment of zebrafish *spp1* (Image clone 5602411, Imagenes) was cloned into pBluescript+ (Stratagene) for RNA probe synthesis. Morpholino oligonucleotides (MOs) (Gene Tools) were dissolved in water and injected at 1 nl per embryo. The *tmem2* MO was targeted to the exon 5 donor site with the sequence 5′-ACAAACCAAAGCCATCTCACCTTGA-3′. The splice-targeting *bmp4* MO was as previously described (Chocron et al., 2007). The standard *p53* control MO from Gene Tools was used.

In situ hybridisation (ISH), immunohistochemistry and sectioning

ISH analysis of zebrafish was carried out as previously described (Smith et al., 2009). For sectioning, embryos were mounted in Technovit 8100 (Hereaus Kulzer) and sectioned at 7 μm. Whole-mount ISH analysis of mouse embryos was as described previously (Fowles et al., 2003). Immunohistochemistry was performed as previously described (Smith et al., 2008). Hyaluronic acid staining was performed on paraffin sections as described previously (Bakkers et al., 2004).

BAC recombineering

BAC recombineering was performed as previously described (Hogan et al., 2009), integrating the Cherry coding sequence in place of the *tmem2* stop codon in CHORI BAC clone CH73-204I21. Primer sequences are detailed in Table S1 in the supplementary material.

Heart rate quantitation

Heartbeats of 15 (alternating) sibling and mutant embryos were counted over a 1-minute period under a dissecting microscope.

Imaging and image analysis

Confocal imaging was performed using Leica SP2 and Zeiss 510 confocal laser-scanning microscopes with 40× magnification. Embryos were mounted in ProLong Gold (Invitrogen). Imaris (Bitplane) (Figs 1, 2) and Volocity (Improvision) (Figs 3, 4) software were used for image analysis. ImageJ software was employed to remove myocardial Alcama expression in Figs 3 and 4. Statistical analyses were performed in Excel (Microsoft).

RESULTS AND DISCUSSION

Identification of the *wkm* mutant

To identify genetic regulators of cardiac morphogenesis and EC development, a forward genetic screen for zebrafish mutants with defective heart looping was performed. Embryos were screened at

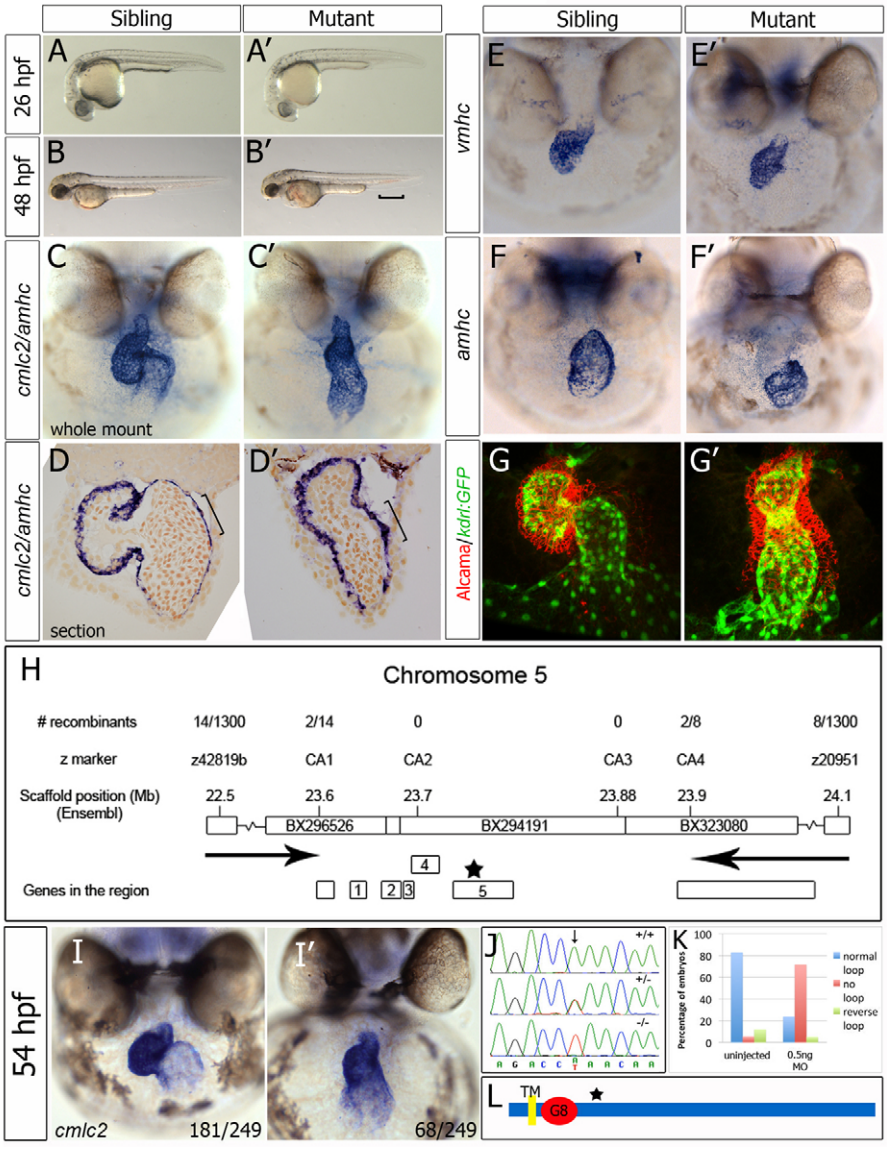

Fig. 1. Zebrafish *wkm*, which is associated with abnormal cardiac looping, encodes the novel protein Tmem2. (**A-B′**) Bright-field images of *wkm* mutants and siblings. The bracket indicates pooling of blood above the ventral tail fin. (**C-D′**) Whole-mount in situ hybridisation (ISH) (C,C′) and sectioning (D,D′) of *wkm* sibling and mutant embryos for *cmlc2* (*myl7*) and *amhc* (*myh6*) at 52 hpf. The bracket indicates elongated atrial cells in siblings but not in mutant embryonic hearts. (**E-F′**) ISH staining for *vmhc* (E,E′) and *amhc* (F,F′) at 52 hpf. (**G**,**G′**) Confocal *z*-stacks of whole-mount Alcama-immunostained (red) *kdrl:GFP* (green) transgenic embryos at 50 hpf. (**H**) Positional cloning of *wkm* (allele *tmem2*^{hu4800}) on zebrafish chromosome 5 (Ensembl, zv8). Arrows indicate the region where the *wkm* mutation resides between. (**I**,**I′**) ISH for *cmlc2* on embryos from a *wkm*^{hu5935} × *wkm*^{hu4800} transheterozygote cross, showing (I) unaffected and (I′) affected transheterozygotes. The number of embryos scored out of the total examined is indicated. (**J**) Exon sequencing revealed an A-to-T transversion (arrow) in the *wkm*^{hu5935} allele, resulting in a stop codon (K329X) in *tmem2*. (**K**) A morpholino (MO) against *tmem2* (0.5 ng) reproduced the *wkm* phenotype in 58/81 injected embryos (72%) at 48 hpf. (**L**) The predicted single transmembrane domain (TM), the G8 domain and the location of the premature stop codon (star, see H) in Tmem2.

26-32 hours post-fertilisation (hpf) to ensure normal formation and asymmetry of the cardiac tube, and at 48-54 hpf, to identify mutants with defective looping. Two alleles of the recessive lethal *wkm* (*wkm*^{hu4800} and *wkm*^{hu5935}) mutation were identified that resulted in mutants that were indistinguishable from siblings at 26 hpf but displayed an unlooped heart at 48 hpf (Fig. 1A-C′). In heterozygous crosses the alleles failed to complement (27% affected transheterozygotes), confirming that these two mutations are allelic (Fig. 1I,I′). The gross morphology of *wkm* mutants was relatively normal, as compared with siblings. The cardiac looping defect was accompanied by cardiac oedema and an accumulation of blood above the ventral tail fin. By 4 days post-fertilisation (dpf), massive pericardial oedema was observed (data not shown) and, from 5 dpf onward, lethality resulted.

wkm mutant hearts fail to undergo looping morphogenesis but appear otherwise normal

The morphology of the heart was examined by in situ hybridisation (ISH) analysis. A reduction in the S-loop shape of the heart accompanied by diminished constriction of the AVC were observed in both whole-mount ISH and frontally sectioned embryos stained for *cardiac myosin light chain 2* (*cmlc2*; also known as *myl7*) and *atrial myosin heavy chain* (*amhc*; also known as *myh6*) (Fig. 1C-D′). Chamber myocardium was specified normally in *wkm* mutants as determined by *ventricular myosin heavy chain* (*vmhc*) and *amhc* expression (Fig. 1E-F′). Pacemaker activity was also unchanged in *wkm* mutants, when beats per minute at 50 hpf were measured in mutant and sibling embryos (see Fig. S1A in the supplementary material). At later stages (>56 hpf), heart rate and cardiac contractility became impaired (data not shown); however, this occurred subsequent to the looping defect and was, therefore, secondary to the morphogenetic defect. No alteration in overall myocardial cell number was observed at 50 hpf in *wkm* mutants as compared with sibling embryos (see Fig. S1B in the supplementary material).

The overall morphology of *wkm* hearts was examined by confocal imaging of embryos immunostained for Alcama [also known as Dm-grasp; which labels the myocardium and ECs (Beis et al., 2005)] on the transgenic background *kdrl:GFP* (GFP expressed in all endocardial cells). The myocardium and endocardium were intact in the *wkm* heart, forming distinct layers. The presence of the endocardium was further confirmed by ISH for *nfatc1* (see Fig. S2 in the supplementary material), and the overall laterality of the embryo was normal, as determined by the direction of gut looping (see Fig. S2 in the supplementary material).

Taken together, these data indicate that myocardial patterning, cell number and function and endocardial specification were unaffected in *wkm* mutants at 50 hpf, suggesting that the cardiac morphogenesis defect was highly specific.

wkm encodes Tmem2, a single-pass transmembrane domain-containing protein

To determine the gene responsible for the *wkm* phenotype, positional cloning using traditional genetic mapping with SSLP markers was performed. The mutation responsible for one of the *wkm* alleles (*wkm*^{hu4800}) was localised to a genetic interval of 0.3 Mb on chromosome 5 containing five genes (Fig. 1H); however, sequencing of the coding regions failed to identify any causative mutations. For the second allele (*wkm*^{hu5935}), linkage on chromosome 5 was confirmed. Sequencing the coding regions of all five genes in the genetic interval for *wkm*^{hu5935} revealed an A-to-T transition at position 985 in the third exon of the 23-exon gene *transmembrane protein 2* (*tmem2*; accession NM_001099449). This mutation is predicted to introduce a stop codon (K329X) leading to a prematurely truncated protein (Fig. 1J). To confirm that the lesion in *tmem2* is responsible for the *wkm* phenotype, morpholino (MO) knockdown of *tmem2* was performed and robustly reproduced the *wkm* cardiac phenotype (Fig. 1K). Thus, genetic linkage, the identification of a premature stop codon and the MO phenocopy confirm that disruption of the *tmem2* gene results in the *wkm* phenotype (see Fig. S3 in the supplementary material).

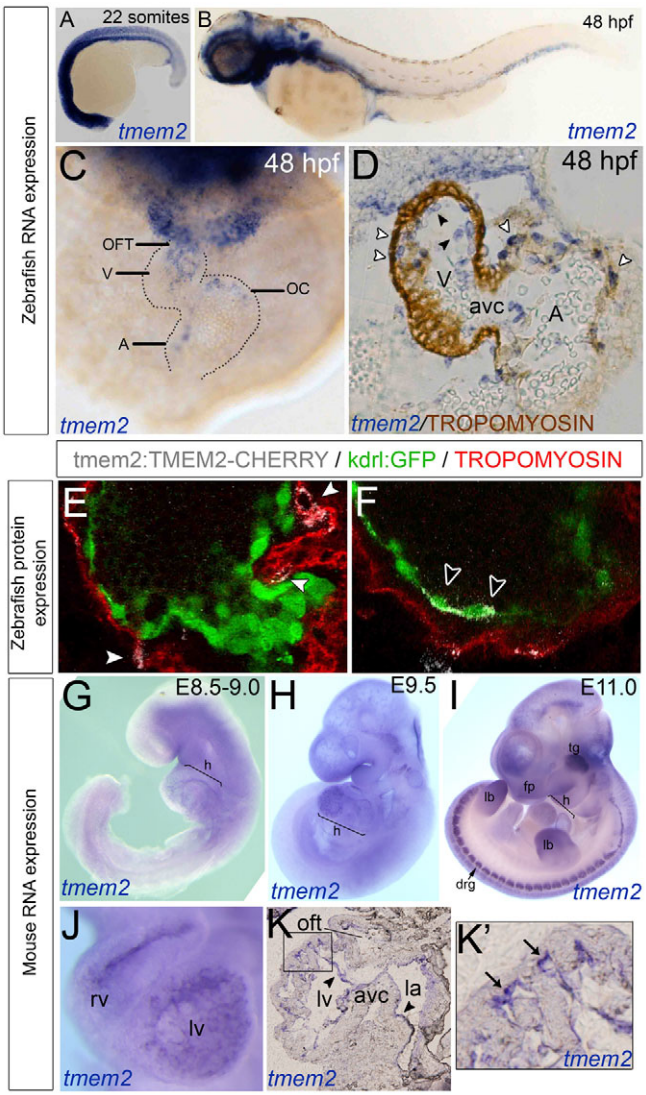

Fig. 2. *tmem2* expression in the endocardial cells of zebrafish and mouse hearts and in the myocardial cells of zebrafish hearts. (**A-C**) ISH for zebrafish *tmem2* expression at 22 somites (A) and 48 hpf (B,C) shown in lateral (A,B) or frontal (C) view. (**D**) Transverse section of *tmem2* ISH with tropomyosin counterstaining. White arrowheads, myocardial *tmem2* expression; black arrowheads, endocardial *tmem2* expression. (**E**,**F**) Transient expression from a Tmem2-Cherry BAC construct. White arrowheads, myocardial Tmem2-Cherry; black arrowheads, endocardial Tmem2-Cherry. (**G-K′**) ISH of mouse embryos stained for *Tmem2* at E8.5-9.0 (G), E9.5 (J-K′) and E11.0 (I). (K) Sagittal sectioning revealed expression in the endocardium (arrows). (K′) Enlargement of boxed region in K. Arrows indicate staining in the ventricular trabeculae. A, atrium; avc, atrioventricular canal; drg, dorsal root ganglion; fp, facial prominences; h, heart; la, left atrium; lb, limb buds; lv, left ventricle; OC, outer curvature; OFT, outflow tract; tg, trigeminal ganglion; V, ventricle.

The 4173 nt *tmem2* transcript is predicted to encode a 1390 amino acid protein that harbours a single transmembrane domain in close proximity to the N-terminus, and a G8 domain, which is hypothesised to be involved in ligand binding and catalysis (Fig. 1L) (He et al., 2006). The long C-terminal region of the protein is predicted to reside extracellularly (Hogan et al., 2003). Until now, no functional role had been ascribed to Tmem2.

Tmem2 is expressed in the developing zebrafish and mouse heart

tmem2 expression was examined in zebrafish and found to be present at the 2-cell stage (data not shown), indicating maternal deposition, and at the 22-somite stage, when it is ubiquitously expressed (Fig. 2A). By 48 hours, expression is restricted to the brain and head mesenchyme, otic vesicles, fin buds, caudal vein and the heart (Fig. 2B). Within the heart, *tmem2*-positive regions included the outflow tract, ventricular regions and outer curvature of the atrium (Fig. 2C). Sectioned hearts counterstained with tropomyosin (to label the myocardium) revealed both myocardial and endocardial expression (Fig. 2D).

To expand on these analyses, a recombineered bacterial artificial chromosome (BAC) containing the *tmem2* locus, with an in-frame insertion of the *cherry* coding sequence replacing the *tmem2* stop codon (resulting in a fusion of Cherry to the Tmem2 C-terminus), was created. Injection of BAC DNA into 1-cell stage zebrafish embryos resulted in mosaic expression of Tmem2-Cherry protein. In the developing heart, fusion protein expression localised to both myocardial and endocardial cells at 48 hpf, consistent with *tmem2* RNA expression at the same stage (Fig. 2E,F). These approaches confirm that *tmem2* is transcribed and expressed in both endocardium and myocardium during morphogenesis of the zebrafish heart.

To investigate possible conservation of function in mammals, we investigated expression of *Tmem2* by whole-mount ISH analysis in mouse embryos. At early stages of development, *Tmem2* showed ubiquitous expression (Fig. 2G,H), although enriched, punctate staining was evident in the developing heart, particularly from E9.5 (Fig. 2J). Sagittal sections of stained E9.5 embryos revealed that expression was restricted to endocardial cells lining the ventricles and atria (Fig. 2K,K′). In an analogous manner to zebrafish *tmem2*, *Tmem2* expression became progressively restricted at later stages of mouse development (E11.0; Fig. 2I).

Although the morphology of zebrafish and mammalian hearts ultimately differ, many of the underlying molecular and cellular patterning events are conserved. The finding that *Tmem2* has enriched expression in the mouse heart suggests a potential conservation of function.

wkm affects cardiac looping via a genetic pathway distinct from *tbx5*

The *tbx5* mutant has been shown to exhibit a specific cardiac looping defect that is similar to *wkm* mutants (Garrity et al., 2002). To determine whether the looping defect observed in *wkm* mutants is related to the *tbx5* genetic pathway, reciprocal expression analysis was performed on both mutants. No obvious difference in *tbx5* expression was observed in *wkm* mutants as compared with sibling embryos (see Fig. S5A,A′ in the supplementary material). Likewise, no difference in *tmem2* expression was observed in *tbx5* mutant embryos (see Fig. S5B,B′ in the supplementary material), suggesting that these genes operate in distinct genetic pathways to affect cardiac looping.

tmem2 is required to restrict endocardial cushion development

To more clearly define the cardiac defect in *wkm* mutants, the expression of a number of regionalised cardiac markers was examined. The myocardial chamber marker *anf* (also known as *nppa*) was expressed in the chambers but excluded from the AVC of *wkm* mutants (Fig. 3A,A′), although the area of *anf*-negative myocardial cells appeared to be broader than in siblings. Strikingly, the myocardial AVC markers *bmp4* and *tbx2b* were upregulated and expanded, with *bmp4* expression notably expanded throughout the entire ventricle in *wkm* mutants (Fig. 3B-C′). As with markers of the AVC myocardium, the AVC endocardial marker *hyaluronan synthase 2* (*has2*) was expanded into the chambers (Fig. 3D,D′). Concordantly, an increase in hyaluronic acid (HA) in the chambers was also observed (see Fig. S5A,A′ in the supplementary material). *notch1b* expression in the AVC was less condensed but otherwise unchanged in mutants (see Fig. S5B,B′ in the supplementary material); however, expression of the Notch target *hey2* was expanded (see Fig. S5C,C′ in the supplementary material). Immunofluorescence analysis of the EC marker Alcama also showed a dramatic expansion in ECs (Fig. 3E,E′), confirming an expansion of the EC region in *wkm* mutants. Intriguingly, whereas

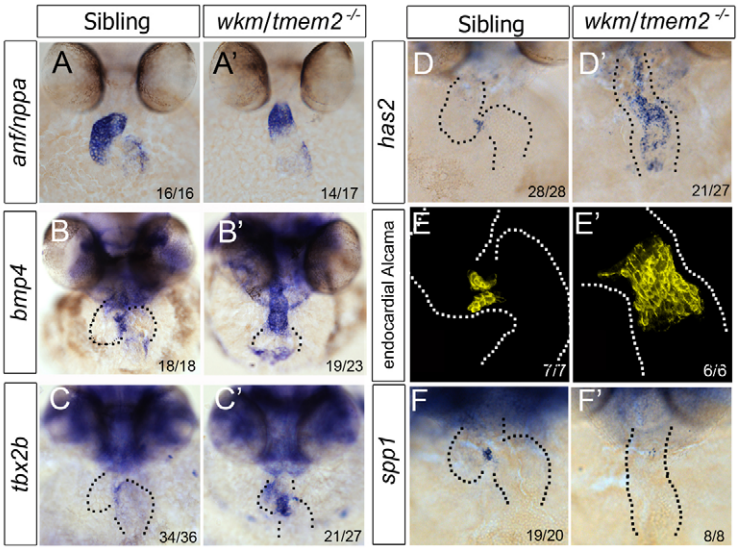

Fig. 3. *tmem2* is required to restrict the AVC. (**A-D′**) ISH for *anf* (A,A′), *bmp4* (B,B′), *tbx2b* (C,C′) and *has2* (D,D′) in zebrafish *wkm* mutants and siblings at 52 hpf. (**E**,**E′**) Three-dimensional projections of endocardial-specific Alcama expression in *wkm* mutants and siblings at 50 hpf. (**F**,**F′**) *spp1* expression in *wkm* mutants and siblings at 50 hpf. Dotted lines outline the morphology of the heart.

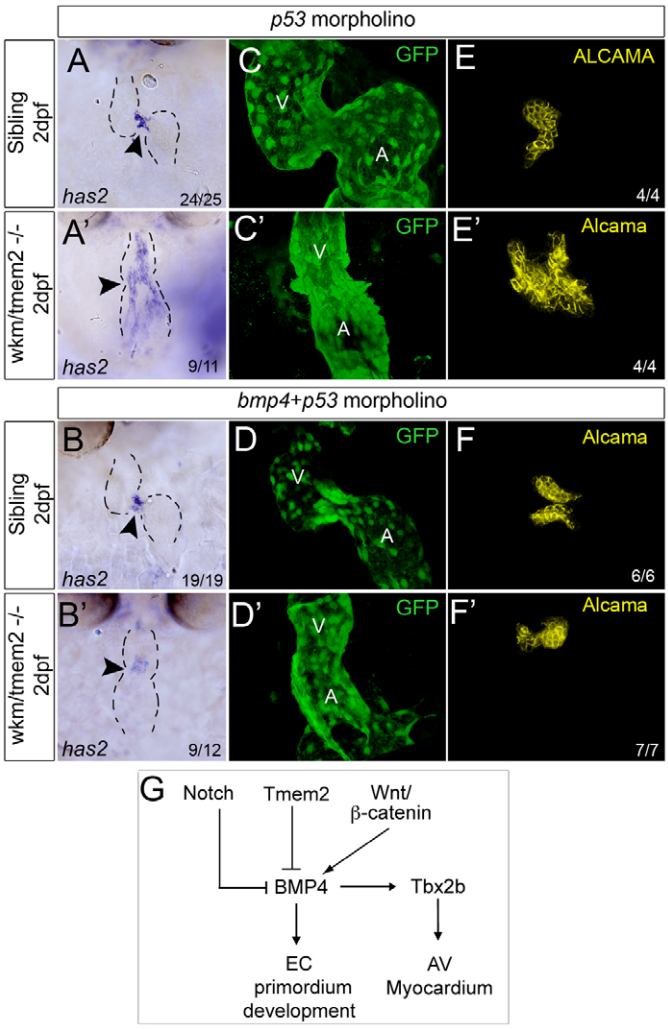

Fig. 4. The endocardial expansion in *wkm* mutants is *bmp4* driven. (**A-B′**) ISH for zebrafish *has2* in *wkm* mutants and siblings injected with *p53* control MO (A) or *p53* MO + *bmp4* MO at 52 hpf and examined at 2 dpf. Dashed lines outline the morphology of the heart. Arrowhead indicates the location of the AVC. (**C-F′**) Endothelial Kdrl:GFP (C-D′) or endocardial Alcama (E-F′) expression in *wkm* mutants and siblings injected with *p53* MO or *p53* MO + *bmp4* MO. (**G**) Model of AVC boundary regulation. In zebrafish, Bmp4 can drive EC primordium development in the AVC. Tmem2 restricts EC formation to the AVC by inhibiting Bmp4. A, atrium; AV, atrioventricular; EC, endocardial cushion; V, ventricle.

the suite of early AVC developmental markers showed expansion in their expression domains, *spp1* (also known as *osteopontin* or *zgc:111821*) showed a substantial reduction in expression (Fig. 3F,F′). *spp1* marks the developing cardiac valves at later stages of formation (Peal et al., 2009), suggesting that, although the EC primordium is expanded, there is a failure to progress to valve maturation.

AVC expansion in *wkm* mutants is driven by Bmp4

Bmp signalling is essential for the formation of the AVC (van Wijk et al., 2007). *bmp2/4* have restricted expression in the AVC and outflow tract and have been demonstrated to promote cardiac jelly formation, epithelial-to-mesenchymal transition and patterning of the AVC (Ma et al., 2005). Given this role, we hypothesised that the ectopic expression of *bmp4* in *wkm* mutants might be responsible for the expanded AVC phenotype. To test this, Bmp4 was depleted in mutant and sibling zebrafish embryos by MO knockdown and ECs examined. *has2* expression was unchanged in sibling and mutant embryos injected with control *p53* MO in that an expansion of *has2* was evident (Fig. 4A). By contrast, whereas injection of *bmp4* MO had no effect on *has2* expression in sibling embryos, rescue of the ectopic expression of *has2* in *wkm* mutants was observed. A similar rescue was observed for Alcama staining in ECs (Fig. 4A), indicating that the expanded EC phenotype in *wkm* mutants is Bmp4 dependent. It is noteworthy that the AVC expression of *has2* and Alcama are not abolished in *bmp4* morphants, suggesting that this region is not under the sole regulation of Bmp4.

The expanded AVC phenotype of *wkm* mutants is phenotypically indistinguishable from the defect seen in zebrafish *tbx5*, *apc* and *hey2* mutants. In these cases, an expansion of *bmp4* expression throughout the ventricular myocardium is observed and is associated with EC marker expansion (Camarata et al., 2010; Garrity et al., 2002; Hurlstone et al., 2003; Rutenberg et al., 2006). Here, we show that, downstream of *tmem2*, ectopic *bmp4* expression is functionally responsible for the expansion of the immature AVC. Bmp signalling is known to activate *tbx2* expression in the AVC (Singh et al., 2009; Yamada et al., 2000) and, in turn, *tbx2* inhibits the chamber myocardial differentiation programme via the repression of genes such as *anf* (Habets et al., 2002). The boundary between the AVC and chambers is kept in check by chamber-specific genes, such as *Hesr1* and *Hesr2* (Kokubo et al., 2007). Clearly, *tbx5*, *apc*, *hey2* and, now, *tmem2* (Fig. 4B) are instrumental in determining this AVC boundary and regionally restricting EC development.

Acknowledgements

We thank the Hubrecht Screen Team and Jeroen Korving for technical assistance and Dr David Pennisi for useful discussions. Confocal microscopy was performed at the ACRF Cancer Biology Imaging Facility at the IMB, established with the generous support of the Australian Cancer Research Foundation (ACRF).

Funding

This work was supported by the Research Council for Earth and Life Sciences (ALW) from the Netherlands Organization for Science (NWO) to J.B. K.A.S. was supported by a UQ Postdoctoral Fellowship, Concordia Fellowship, an Institute for Molecular Bioscience (IMB) Development Grant and National Health and Medical Research Council (NHMRC) of Australia Project Grant. B.M.H. is an Australian Research Council (ARC) Future Fellow and C.W. is a NHMRC Senior Research Fellow.

Competing interests statement

The authors declare no competing financial interests.

Supplementary material

Supplementary material for this article is available at
http://dev.biologists.org/lookup/suppl/doi:10.1242/dev.065375/-/DC1

References

Bakkers, J., Kramer, C., Pothof, J., Quaedvlieg, N. E., Spaink, H. P. and Hammerschmidt, M. (2004). Has2 is required upstream of Rac1 to govern dorsal migration of lateral cells during zebrafish gastrulation. *Development* **131**, 525-537.

Beis, D., Bartman, T., Jin, S. W., Scott, I. C., D'Amico, L. A., Ober, E. A., Verkade, H., Frantsve, J., Field, H. A., Wehman, A. et al. (2005). Genetic and cellular analyses of zebrafish atrioventricular cushion and valve development. *Development* **132**, 4193-4204.

Camarata, T., Krcmery, J., Snyder, D., Park, S., Topczewski, J. and Simon, H. G. (2010). Pdlim7 (LMP4) regulation of Tbx5 specifies zebrafish heart atrio-ventricular boundary and valve formation. *Dev. Biol.* **337**, 233-245.

Chi, N. C., Shaw, R. M., De Val, S., Kang, G., Jan, L. Y., Black, B. L. and Stainier, D. Y. (2008). Foxn4 directly regulates tbx2b expression and atrioventricular canal formation. *Genes Dev.* **22**, 734-739.

Chocran, S., Verhoeven, M. C., Rentzsch, F., Hammerschmidt, M. and Bakkers, J. (2007). Zebrafish Bmp4 regulates left-right asymmetry at two distinct developmental time points. *Dev. Biol.* **305**, 577-588.
Fowles, L. F., Bennetts, J. S., Berkman, J. L., Williams, E., Koopman, P., Teasdale, R. D. and Wicking, C. (2003). Genomic screen for genes involved in mammalian craniofacial development. *Genesis* **35**, 73-87.
Garrity, D. M., Childs, S. and Fishman, M. C. (2002). The heartstrings mutation in zebrafish causes heart/fin Tbx5 deficiency syndrome. *Development* **129**, 4635-4645.
Habets, P. E., Moorman, A. F., Clout, D. E., van Roon, M. A., Lingbeek, M., van Lohuizen, M., Campione, M. and Christoffels, V. M. (2002). Cooperative action of Tbx2 and Nkx2.5 inhibits ANF expression in the atrioventricular canal: implications for cardiac chamber formation. *Genes Dev.* **16**, 1234-1246.
He, Q. Y., Liu, X. H., Li, Q., Studholme, D. J., Li, X. W. and Liang, S. P. (2006). G8: a novel domain associated with polycystic kidney disease and non-syndromic hearing loss. *Bioinformatics* **22**, 2189-2191.
Hogan, B. M., Bos, F. L., Bussmann, J., Witte, M., Chi, N. C., Duckers, H. J. and Schulte-Merker, S. (2009). Ccbe1 is required for embryonic lymphangiogenesis and venous sprouting. *Nat. Genet.* **41**, 396-398.
Hogan, M. C., Griffin, M. D., Rossetti, S., Torres, V. E., Ward, C. J. and Harris, P. C. (2003). PKHDL1, a homolog of the autosomal recessive polycystic kidney disease gene, encodes a receptor with inducible T lymphocyte expression. *Hum. Mol. Genet.* **12**, 685-698.
Huang, C. J., Tu, C. T., Hsiao, C. D., Hsieh, F. J. and Tsai, H. J. (2003). Germ-line transmission of a myocardium-specific GFP transgene reveals critical regulatory elements in the cardiac myosin light chain 2 promoter of zebrafish. *Dev. Dyn.* **228**, 30-40.
Hurlstone, A. F., Haramis, A. P., Wienholds, E., Begthel, H., Korving, J., Van Eeden, F., Cuppen, E., Zivkovic, D., Plasterk, R. H. and Clevers, H. (2003). The Wnt/beta-catenin pathway regulates cardiac valve formation. *Nature* **425**, 633-637.
Kokubo, H., Tomita-Miyagawa, S., Hamada, Y. and Saga, Y. (2007). Hesr1 and Hesr2 regulate atrioventricular boundary formation in the developing heart through the repression of Tbx2. *Development* **134**, 747-755.
Lagendijk, A., Smith, K. and Bakkers, J. (2010). Genetics of congenital heart defects: a candidate gene approach. *Trends Cardiovasc. Med.* **20**, 124-128.
Lawson, N. D. and Weinstein, B. M. (2002). In vivo imaging of embryonic vascular development using transgenic zebrafish. *Dev. Biol.* **248**, 307-318.
Ma, L., Lu, M. F., Schwartz, R. J. and Martin, J. F. (2005). Bmp2 is essential for cardiac cushion epithelial-mesenchymal transition and myocardial patterning. *Development* **132**, 5601-5611.
Mably, J. D., Mohideen, M. A., Burns, C. G., Chen, J. N. and Fishman, M. C. (2003). heart of glass regulates the concentric growth of the heart in zebrafish. *Curr. Biol.* **13**, 2138-2147.
Moorman, A. F. and Christoffels, V. M. (2003). Cardiac chamber formation: development, genes, and evolution. *Physiol. Rev.* **83**, 1223-1267.
Peal, D. S., Burns, C. G., Macrae, C. A. and Milan, D. (2009). Chondroitin sulfate expression is required for cardiac atrioventricular canal formation. *Dev. Dyn.* **238**, 3103-3110.
Rutenberg, J. B., Fischer, A., Jia, H., Gessler, M., Zhong, T. P. and Mercola, M. (2006). Developmental patterning of the cardiac atrioventricular canal by Notch and Hairy-related transcription factors. *Development* **133**, 4381-4390.
Singh, R., Horsthuis, T., Farin, H. F., Grieskamp, T., Norden, J., Petry, M., Wakker, V., Moorman, A. F., Christoffels, V. M. and Kispert, A. (2009). Tbx20 interacts with smads to confine tbx2 expression to the atrioventricular canal. *Circ. Res.* **105**, 442-452.
Smith, K. A., Chocron, S., von der Hardt, S., de Pater, E., Soufan, A., Bussmann, J., Schulte-Merker, S., Hammerschmidt, M. and Bakkers, J. (2008). Rotation and asymmetric development of the zebrafish heart requires directed migration of cardiac progenitor cells. *Dev. Cell* **14**, 287-297.
Smith, K. A., Joziasse, I. C., Chocron, S., van Dinther, M., Guryev, V., Verhoeven, M. C., Rehmann, H., van der Smagt, J. J., Doevendans, P. A., Cuppen, E. et al. (2009). Dominant-negative ALK2 allele associates with congenital heart defects. *Circulation* **119**, 3062-3069.
Timmerman, L. A., Grego-Bessa, J., Raya, A., Bertran, E., Perez-Pomares, J. M., Diez, J., Aranda, S., Palomo, S., McCormick, F., Izpisua-Belmonte, J. C. et al. (2004). Notch promotes epithelial-mesenchymal transition during cardiac development and oncogenic transformation. *Genes Dev.* **18**, 99-115.
van Wijk, B., Moorman, A. F. and van den Hoff, M. J. (2007). Role of bone morphogenetic proteins in cardiac differentiation. *Cardiovasc. Res.* **74**, 244-255.
Walsh, E. C. and Stainier, D. Y. (2001). UDP-glucose dehydrogenase required for cardiac valve formation in zebrafish. *Science* **293**, 1670-1673.
Westerfield, M. (1995). *The Zebrafish Book – A Guide for Laboratory Use of Zebrafish (Brachydanio rerio)*. Eugene, Oregon: University of Oregon Press.
Wienholds, E., Schulte-Merker, S., Walderich, B. and Plasterk, R. H. (2002). Target-selected inactivation of the zebrafish rag1 gene. *Science* **297**, 99-102.
Yamada, M., Revelli, J. P., Eichele, G., Barron, M. and Schwartz, R. J. (2000). Expression of chick Tbx-2, Tbx-3, and Tbx-5 genes during early heart development: evidence for BMP2 induction of Tbx2. *Dev. Biol.* **228**, 95-105.